Towards a better understanding of the combustion of oxygenated aromatic hydrocarbons. Comparing benzene, toluene, phenol and anisole with ignition delay times in a rapid compression machine

R. D. Büttgen*[,1], L. Pratali Maffei[2], M. Pelucchi[2], T. Faravelli[2], A. Frassoldati[2], K. A. Heufer[1]

[1]Physico Chemical Fundamentals of Combustion (PCFC), RWTH Aachen University, Schinkelstraße 8, 52062 Aachen, Germany

[2]CRECK Modeling Lab – Department of Chemistry, Materials and Chemical Engineering, Politecnico di Milano, 20133 Milano, Italy

Abstract

Ignition delay times (IDTs) of the oxygenated aromatic hydrocarbons (OAHCs) anisole ($C_6H_5OCH_3$) and phenol (C_6H_5OH) and the analogues non-oxygenated aromatic hydrocarbons (AHCs) toluene ($C_6H_5CH_3$) and benzene (C_6H_6) have been measured in the PCFC rapid compression machine (RCM) at stoichiometric, fuel-in-air conditions. With the two targeted compression pressures (p_c) of 1 and 2 MPa a temperature range of 870 to 1100 K was covered. The IDTs of all four molecules revealed an Arrhenius behavior. The different reactivity can be ranked as the following, starting with the lowest reactivity: benzene < toluene < phenol < anisole. Literature available models containing anisole and phenol have been used to simulate the IDTs of *this study* highlighting discrepancies in both, model to experiment and model to model accordance. Finally, the CRECK mechanism was used to conduct rate-of-production (ROP) and sensitivity analysis to gain insight into the combustion of OAHCs and highlight interconnections and shortcomings of OAHCs.

1. Introduction

With the ever-growing demand for energy and propulsion, the ecological demand to lower emissions and the economical demand to increase efficiency, the necessity to find suitable fuel alternatives emerges. Further, future bio-fuels should not interfere with food stock [1, 2]. A potential biomass feed stock fulfilling those requirements is lignin. It is one of the most abundant resource of renewable oxygenated aromatic hydrocarbons (OAHCs) [3, 4]. The complex structure of lignin bears the potential for a variety of OAHCs like anisole, phenol, guaiacol [5, 6] and non-oxygenated aromatic hydrocarbons (AHCs) such as benzene [7].

Besides the reduced CO_2-footprint of bio-derived fuel or fuel/bio-fuel blends, the OAHCs are also capable of increasing the fuel quality as octane boosters and thereby increasing the efficiency in downsized, turbocharged engines [8]. Comparing the research octane numbers (RON) of ethanol (108) [9] and anisole (120) [10] the potential to improve gasoline fuels is further highlighted. Besides anisole, other possible lignin based OAHCs also have impressive RON, e.g. 4-methylanisole (166) and *p*-cresol (153) [11]. For phenol, no RON is currently available in literature, but as the results of this study indicate, a similar high value is expected. This highlights that multiple products based on lignin have the potential to be used as a fuel component.

However, current knowledge of combustion of OAHCs is limited. Especially the literature about phenol in combustion is scarce. For anisole jet stirred reactor experiments and laminar flow reactor experiments are available in literature [10, 12, 13] at low pressures up to 0.1 MPa. Thus in *this study*, anisole and phenol are investigated by measuring their ignition delay times (IDTs) in the PCFC RCM at compressed pressures (p_c) of 1 and 2 MPa for stoichiometric fuel-in-air conditions ($\phi = 1$) for the first time. Coherent to this dataset, the non-oxygenated chemical analogues benzene and toluene are tested at the same conditions enabling a direct comparison of their ignition delay times (IDT). Benzene and Toluene have been chosen because they are the direct non-oxygenated equivalent of the oxygenates investigated and benzene is also a possible lignin based product [7]. In Figure 1 details of the investigated species are shown highlighting their similarities.

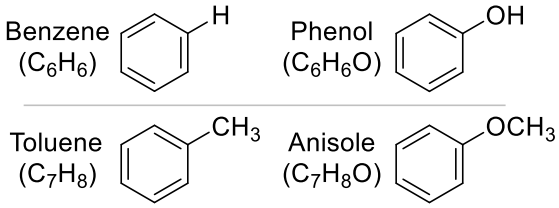

Figure 1: Preferred IUPAC names, skeletal formula and sum formula (in brackets) of the investigated molecules.

Analyzing the reaction pathway scheme of both benzene and anisole, it is apparent that for both molecules phenoxy and phenol are important combustion intermediates. However, most probably due to the scarcity of experimental data and to a vague definition of relevant reaction classes for AHCs and OAHCs, no dedicated phenol models have been systematically developed and presented in the literature. For anisole a few dedicated models have been published recently [10, 12]. The JSR speciation results of Nowakowska et al. [12] shows that phenol is a major intermediate formed in the combustion of anisole, indicating that an anisole model should also be capable of predicting pure phenol data reasonably well. Currently only the essential reaction pathways for phenol are implemented in comprehensive kinetic models such as AramcoMech 3.0 [14] (C_0-benzene), Livermore [15] (C_0-real fuels) and

* Corresponding author: buettgen@pcfc.rwth-aachen.de

CRECK [16] (C_0-real fuels-PAHs and soot). Pelucchi et al. [17] recently presented a first systematic assessment of oxygenated aromatic species kinetics, moving from single substituted aromatics (phenol and anisole) up to catechol, guaiacol and vanillin. Two dedicated anisole models [10, 12] and the CRECK mechanism [17] have been used to simulate the IDT results of *this study* of anisole and phenol. Further, the CRECK model has been adopted to interpret the experimental results, highlighting important reaction pathways by means of rate-of-production (ROP) and sensitivity analyses.

2. Experimental

The RCM used in this study has been described in detail in a previous work [18] and will be briefly reiterated herein. The PCFC RCM has a single creviced piston configuration with a variable end wall to cover a wide range of compression ratios. The RCM and the attached manifold including the mixing tanks are equipped with a heating system and are completely thermally insolated ensuring a homogenous temperature distribution from ambient temperatures up to 150 °C. The mixture and experiment preparation are conducted by measuring the pressure in the system with two static pressure sensors (STS PTM/RS485) suited for up to 50 kPa and 500 kPa, respectively. The dynamic pressure in the experiment is measured with the Kistler 6125CU20. The compressed temperature (T_c) is calculated assuming an isentropic compression as described in [19]. Corresponding to the reactive experiments, non-reactive experiments are conducted as shown in Figure 2. In the non-reactive experiments, the oxygen is replaced by nitrogen to obtain a mixture with similar heat capacity and to avoid the exothermicity.

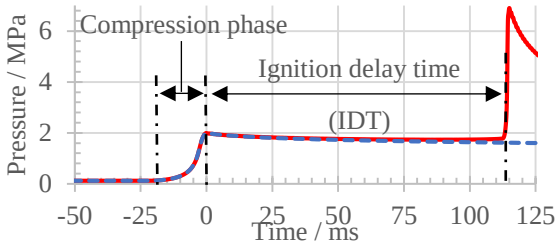

Figure 2: Reactive (red, solid) and non-reactive (blue, dashed) traces of a 1 MPa phenol RCM experiment.

These non-reactive experiments are then taken to obtain time-resolved effective volume profiles used for simulations. This modeling approach has been described in more detail in literature [19-21]. Anisole, phenol, benzene and toluene were obtained by Merck with a purity of at least 99.8%. Oxygen (99.999 %), and argon (≥ 99.996 %) were obtained by Westfalen AG. All experiments are conducted at stoichiometric, fuel-in-air conditions, $p_c = 1$ and $p_c = 2\ MPa$.

3. Experimental Results

The measured IDTs reveal an Arrhenius behavior for all molecules. A general trend in reactivity can be observed (Figure 3) ranking the fuels in reactivity as follows starting with the lowest reactivity:

Benzene < toluene < phenol < anisole

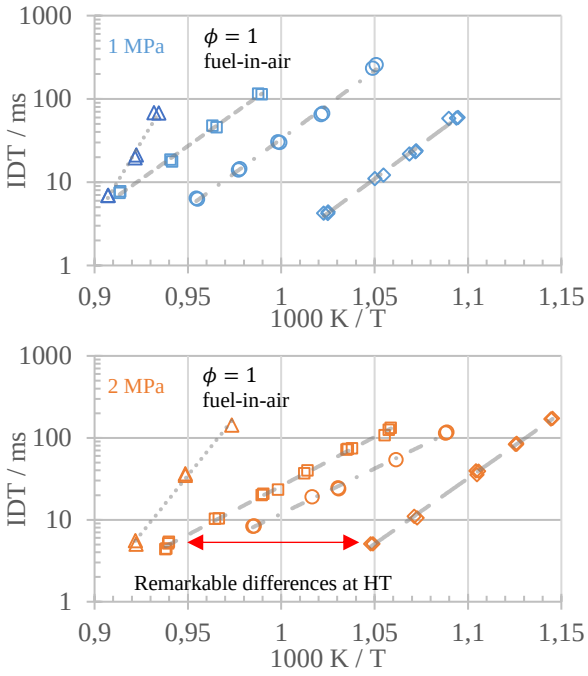

Figure 3: RCM IDTs of anisole (diamonds), phenol (circles), toluene (squares) and benzene (triangle). Red arrows highlighting the differences between benzene/toluene/phenol and anisole. In grey: logarithmic trend lines for each fuel.

All investigated molecules show a strong temperature dependency or apparent activation energy (AAE; $(d(IDT))/dT$), with benzene having the highest AAE. The differences in reactivity and AAE can be explained by analyzing the competing initial reactions, namely the unimolecular decomposition (UD) and the H-atom abstractions (HAA), considering the bond dissociation energies (BDE) and possible resonance stabilization (RS). In general, the UD plays a significant role at high temperatures. In contrast, the HAA influences the combustion from low to high temperatures. For linear hydrocarbons the UD usually occurs by a C-C bond scission as these are the weakest bond (see Figure 4) in linear alkanes.

In the aromatic system however, the C-C BDEs are significantly higher exceeding 500 kJ/mol for aromatic C-C bonds and at least 418 kJ/mol for bonds adjacent to the ring for the investigated molecules. This indicates that UD reactions for benzene, toluene, and phenol are unlikely to play a major role in their reactivity at the investigated temperatures. In contrast, anisole has an additional position for an UD reaction (C-O bond scission) with only 270 kJ/mol. In consequence, the activation energy for this bond scission is drastically lower compared to benzene, toluene, and phenol contributing to the observed higher reactivity of anisole (see Figure 3, red arrows). To further explain the differences in reactivity, the HAA reactions and the RS in the corresponding formed products need to be discussed. Comparing the C-H and O-H BDEs, respectively (Figure 4) it is apparent that phenol and toluene have the lowest C-H/O-H BDE indicating that H-atom abstractions is more favorable for those molecule.

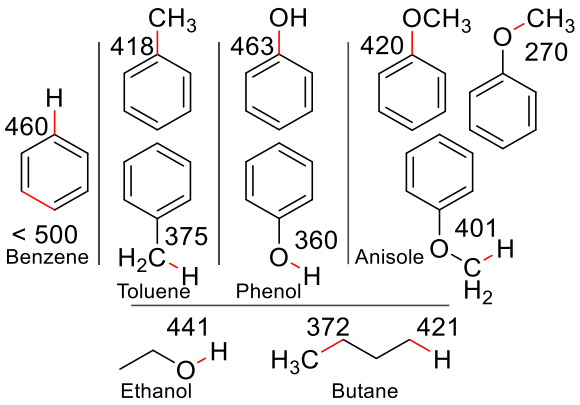

Figure 4: BDE of different bonds (red) in benzene [22], toluene [22], phenol [17], anisole [17] ethanol[23] and butane [23]. All values in kJ/mol.

Especially the phenol O-H bond compared to linear O-H bonds (see Fig. 4.) is remarkably low. However, this would indicate that phenol and toluene should be more reactive, compared to anisole. On the first glance this is in contradiction to the IDTs, but looking at the formed products both toluene and phenol produce a resonance stabilized radical, while the dominant HAA reaction for anisole results in an isolated radical (see Figure 5).

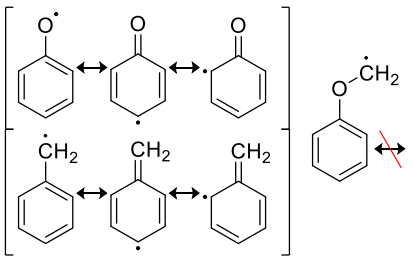

Figure 5: Resonance structure of phenoxy (top) and benzyl radical (bottom). In contrast, the anisyl radical, not capable of resonance stabilization

The RS leads to a less reactive radical than the anisyl radical, explaining the differences in reactivity for the low to high temperatures. Lastly, the low reactivity of benzene can be explained by the fact that for both reactions, the UD and the HAA, the corresponding BDEs are the highest of all investigated molecules.

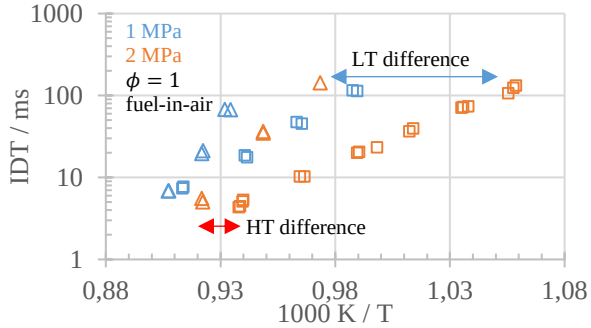

Figure 6: RCM IDTs of Benzene (triangles) and Toluene (squares).

Comparing benzene and toluene, it is apparent that toluene, due to the above described HAA reaction leads to faster ignition at lower temperatures then benzene (LT differences, see Figure 6). At higher temperatures (above 1075 K; 0.93 K^{-1}) enough energy is available for the benzene to overcome the high reaction barriers and initially form the very reactive phenyl radical ($\dot{C}_6H_5$), which is more reactive compared to the resonance stabilized toluene radical ($C_6H_5\dot{C}H_2$). This leads to the strong increase in reactivity of benzene compared to toluene (HT differences, see Figure 6).

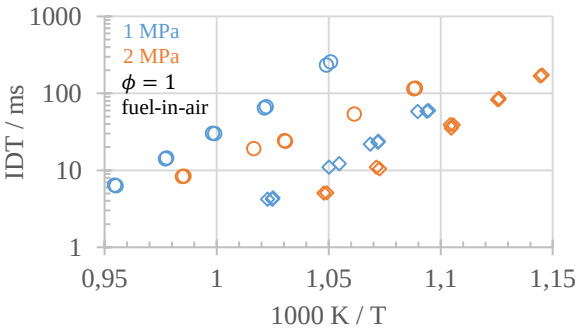

Figure 7: RCM IDTs of Anisole (diamonds) and Phenol (circles).

For anisole and phenol no such differences is observed as both species can undergo reactions at lower temperatures and both form similar reactive products, as highlighted in *Figure 8*. Comparing the pressure dependency, a similar pressure dependency for all four fuels is apparent. With increased pressure, the reactivity of all increases similar (see *Figure 6* and *Figure 7*).

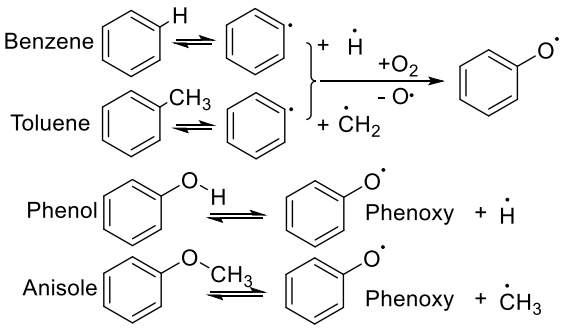

Figure 8: Reaction scheme of the unimolecular decomposition of benzene, toluene, phenol and anisole.

Comparing the potential UD reactions of all 4 species (see Figure 8), it is of interest, that benzene and toluene both form a phenyl radical, which in an consecutive oxidation can form phenoxy. The UD products of phenol and anisole lead also to phenoxy, hence highlighting the potential interconnections of several aromatic molecules.

4. Kinetic Models

The RCM experimental results for anisole and phenol have been used to benchmark three kinetic models [10, 12, 17]. All simulations used effective-volume profiles.

4.1 Anisole Simulations

The experimental IDTs and simulation results for anisole at p_c = 1 and 2 MPa at stoichiometric fuel-in-air conditions are shown in Figure 9.

The model by Nowakowska et al. [12] shows good agreement for the $p_c = 2$ MPa experiments, but is not able to reflect the pressure dependence accurately.

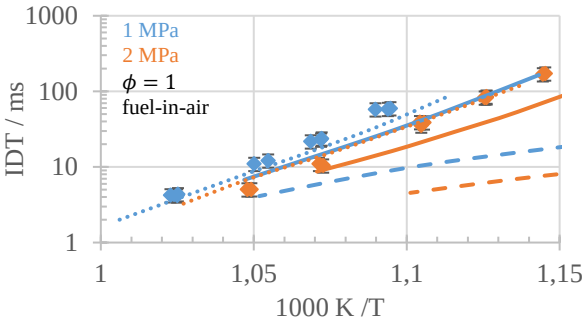

Figure 9: RCM IDTs of Anisole (symbols) and simulations (lines) Simulation results: Dotted: Nowakowska et al. [12, 17]/ Dashed: Wagnon et al. [10]/ Solid: CRECK Model [17].

The model by Wagnon et al. over predicts the reactivity by one order of magnitude, with the biggest deviation towards lower temperatures in both investigated p_c. It is interesting, that although the model by Wagnon et al. shares a common set of validation targets from Nowakowska et al., both model produce different results for the RCM simulations. The CRECK mechanism is capable of predicting the AAE (slope), but over predicts the reactivity for both pressures roughly by a factor of 2.

4.2 Phenol Simulations

Provided that anisole and phenol produce phenoxy radicals as a primary fuel decomposition product, the models also have been benchmarked against the phenol data of *this study*. RCM IDTs and simulations are shown in Figure 10. In contrast to the good agreement of the Nowakowska et al. model with the anisole experiments, phenol reactivity is strongly underpredicted for both pressures. For the 2 MPa conditions only the simulation for the hottest condition lead to a result in the simulation, as depicted by a single dash in Figure 10. For any other cases, no ignition was obtained by the simulation, even when increasing the simulation time to 1000 ms. Analyzing the Nowakowska et al. model, the unimolecular decomposition of phenol to phenoxy and hydrogen is missing. This might be the explanation, why this model predicts a very low reactivity for phenol.

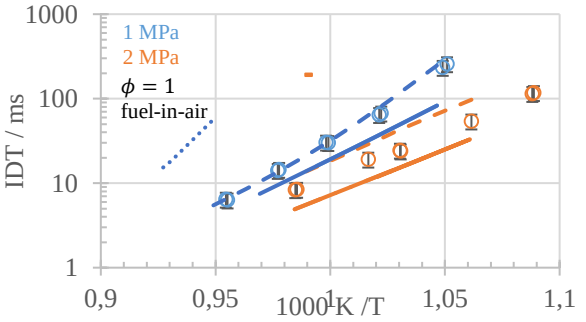

Figure 10: RCM IDTs of Phenol (symbols) and simulations (lines). Simulation results: Dotted: Nowakowska et al. [12] / Dashed: Wagnon et al. [10] / Solid: CRECK Model [17].

The model by Wagnon et al. is capable to predict the phenol IDTs reasonable well, only under predicting the reactivity for the 2 MPa experiments. This could indicate, that the reaction leading to the deviation for the anisole prediction has to be an anisole specific reaction. The CRECK model again does over predict the reactivity with a similar deviation as in anisole.

5. Kinetic Analysis – CRECK Mechanism

To obtain a first insight on the individual reaction steps occurring for phenol and anisole, the CRECK mechanism was used to conduct a rate-of-production (ROP) analysis and a sensitivity analysis. *Figure 11* shows the ROP analysis for stoichiometric phenol and anisole/ air mixtures at $p_c = 2$ MPa and 950 K. 20% fuel conversion were considered in both cases, corresponding to ~ 4 ms residence time of an adiabatic constant volume simulation in the case of anisole and ~ 9 ms residence time for the less reactive phenol.

Phenol is mostly consumed through H-atom abstraction reactions (~52%) by $\dot{O}H$ and $H\dot{O}_2$ to form a resonance stabilized phenoxy radical. It recombines with H atom producing phenol (~14%), or decomposes to cyclopentadiene and CO by a well-skipping recombination with $\dot{H}$ atoms (~16%) [24].

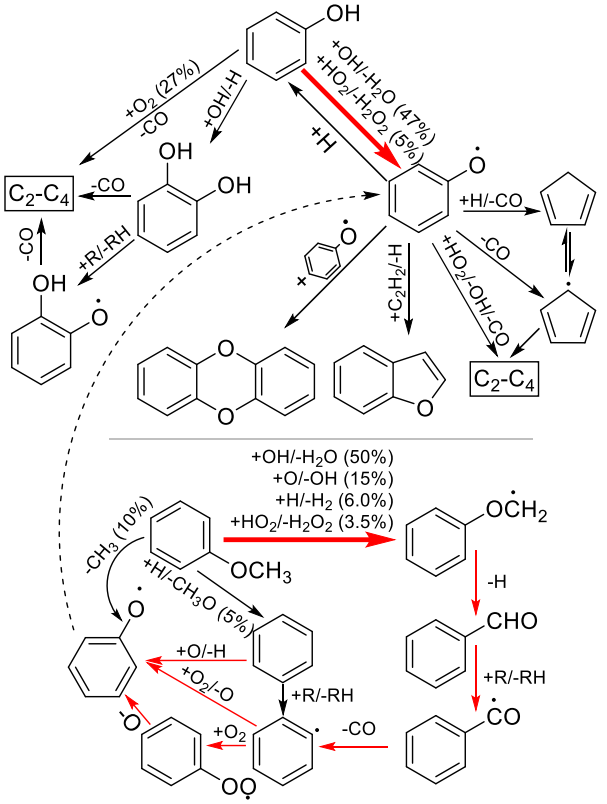

Figure 11: Rate of production analysis of phenol/air (top) and anisole/air (bottom) mixtures at $p_c = 2$ MPa and $T_c = 950$ K, and 20% fuel consumption. Most dominant reaction path highlighted in red.

Recombination of phenoxy radicals form dibenzofuran (~15%), while benzofuran can also be formed via C_2H_2 addition/H elimination (~11%). Due to the resonance stabilization, phenoxy radical can also abstract (~10% total) from stable intermediate species (e.g. CH_2O). The importance of accounting for H-atom abstractions by phenoxy radical has already been discussed in the recent work of Pelucchi et al. [17]. Phenoxy radical decomposition to CO and

cyclopentadienyl ($\dot{C}_5H_5$) only accounts for a few percentages (<5%) at the present conditions. From the work of Saggese et al. [25] interactions with O_2 forming unsaturated C_2-C_4 products through CO elimination and ring opening, were also included as lumped steps to better match speciation experiments.

These pathways account for ~27% of the total flux. Ipso-addition reaction leading to catechol formation are responsible for ~8% of fuel consumption. Catechol decomposes mostly through H-atom abstractions and CO elimination as discussed in [17]. ~75% of anisole is consumed through H-atom abstractions from methoxy, forming anisyl radical ($C_6H_5O\dot{C}H_2$). $\dot{O}H$ and $\dot{O}$ play the major role (50 and 15% respectively), followed by $\dot{H}$ and $H\dot{O}_2$. The anisyl radical thus obtained entirely isomerizes to $C_6H_5CH_2\dot{O}$, that decomposes via β-scission to benzaldehyde and $\dot{H}$. Benzaldehyde is mostly consumed by H-atom abstractions leading to a carbonyl radical rapidly decomposed to phenyl radical and CO. The importance of H-atom abstraction by O(^{3}P) is related to the secondary chemistry of phenyl radical. Interactions with O_2 produce phenyl-peroxy radical that decomposes to phenoxy radical and O(^{3}P).

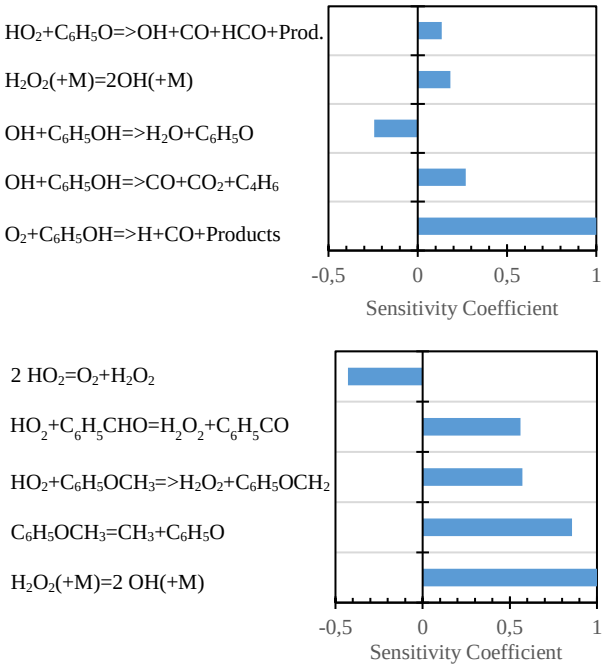

Figure 12: Sensitivity analysis of phenol and anisole in air mixtures at $p_c = 1\ MPa$ and 950 K. A positive coefficient stands for a reaction enhancing ignition and vice versa.

A direct pathway is also kinetically possible, giving the same products. The competing pathways of phenoxy radical previously highlighted for phenol/air mixtures, lead to the formation of lower molecular weight products. From the above analysis the existence of a strong interconnection between phenol and anisole is clearly highlighted.

Figure 12 depicts a sensitivity analysis of rate constants in the CRECK kinetic model for IDTs of phenol and anisole. The simulation conditions are the same as in the reaction path analysis above. Coefficients are normalized over the most sensitive reaction. In the case of phenol the direct interaction with O_2 forming CO and C_2-C_4 products, is the most important reaction. This observation highlights the need of further investigating the potential energy surface of O_2+phenol system, starting from H-atom abstractions leading to $H\dot{O}_2$ and phenoxy. The importance of similar pathways have been already discussed in previous studies [26, 27]. H-atom abstraction by $\dot{O}H$ on phenol shows a negative sensitivity coefficient as it gives rise to the production of resonance stabilized phenoxy radical. The reaction of phenoxy with $H\dot{O}_2$ restoring $\dot{O}H$ shows instead a positive effect on ignition delay times. The low activation energy UD reaction of anisole forming methyl and phenoxy radicals plays a major role as radical pool initiator, followed by H-atom abstractions by $H\dot{O}_2$ from both anisole and benzaldehyde. These pathways produce H_2O_2 whose successive decomposition produces two $\dot{O}H$ radicals. $H\dot{O}_2$ recombination acts as a terminating step, competing with the enhancing effect of H-atom abstractions by $H\dot{O}_2$ and therefore inhibiting the reactivity.

6. Conclusions

Motivated by the strong recent interest in oxygenated aromatics, this work presents a systematic experimental investigation of OAHCs (phenol and anisole) and AHCs (benzene and toluene) ignition delay time in a rapid compression machine at $p_c = 1\ and\ 2\ MPa$ for stoichiometric fuel-in-air conditions. The anisole and phenol IDTs have been used to benchmark recent models. Further, the CRECK mechanism was used to highlight relevant reaction pathways and current shortcomings in the description of OAHCs combustion chemistry. This systematic coupling of new experimental data and kinetic interpretation highlights the expected strong interconnection between phenol, anisole, toluene and benzene motivating further investigations to better assess relevant reaction classes and reference rate parameters of aromatic fuels.

7. Acknowledgements

The authors from PCFC RWTH Aachen University gratefully acknowledge the German Research Foundation (DFG) for financial support for this research provided (HE 7599/1-1).

The authors from Politecnico di Milano gratefully acknowledge the financial support for this research provided by the European Union under the Horizon 2020 research and innovation programme (Residue2Heat project, G.A. No 654650).

8. References

[1] D. Pimentel, Biofuel Food Disasters and Cellulosic Ethanol Problems, 29 (2009) 205-212.

[2] M. Richardson, P. Kumar, Critical Zone services as environmental assessment criteria in intensively managed landscapes, 5 (2017) 617-632.

[3] H. Wang, Y. Pu, A. Ragauskas, B. Yang, From lignin to valuable products–strategies, challenges, and prospects, Bioresour. Technol. 271 (2019) 449-461.

[4] V.K. Thakur, M.K. Thakur, P. Raghavan, M.R. Kessler, Progress in Green Polymer Composites from

Lignin for Multifunctional Applications: A Review, ACS Sustain. Chem. Eng. 2 (2014) 1072-1092.
[5] J. Zhang, L. Lombardo, G. Gözaydın, P.J. Dyson, N. Yan, Single-step conversion of lignin monomers to phenol: Bridging the gap between lignin and high-value chemicals, Chin. J. Catal 39 (2018) 1445-1452.
[6] R.C. Runnebaum, T. Nimmanwudipong, D.E. Block, B.C. Gates, Catalytic conversion of compounds representative of lignin-derived bio-oils: a reaction network for guaiacol, anisole, 4-methylanisole, and cyclohexanone conversion catalysed by Pt/γ-Al2O3, Catal. Sci. Technol. 2 (2012) 113-118.
[7] X.-p. Wu, M.-h. Fan, Q.-x. Li, Production of Benzene from Lignin through Current Enhanced Catalytic Conversion, 30 (2017) 479-486.
[8] M. Tian, R.L. McCormick, M.A. Ratcliff, J. Luecke, J. Yanowitz, P.-A. Glaude, M. Cuijpers, M.D. Boot, Performance of lignin derived compounds as octane boosters, Fuel 189 (2017) 284-292.
[9] M. Eyidogan, A.N. Ozsezen, M. Canakci, A. Turkcan, Impact of alcohol–gasoline fuel blends on the performance and combustion characteristics of an SI engine, Fuel 89 (2010) 2713-2720.
[10] S.W. Wagnon, S. Thion, E.J.K. Nilsson, M. Mehl, Z. Serinyel, K. Zhang, P. Dagaut, A.A. Konnov, G. Dayma, W.J. Pitz, Experimental and modeling studies of a biofuel surrogate compound: laminar burning velocities and jet-stirred reactor measurements of anisole, Combust. Flame 189 (2018) 325-336.
[11] R.L. McCormick, M.A. Ratcliff, E. Christensen, L. Fouts, J. Luecke, G.M. Chupka, J. Yanowitz, M. Tian, M. Boot, Properties of Oxygenates Found in Upgraded Biomass Pyrolysis Oil as Components of Spark and Compression Ignition Engine Fuels, Energy & Fuels 29 (2015) 2453-2461.
[12] M. Nowakowska, O. Herbinet, A. Dufour, P.-A. Glaude, Detailed kinetic study of anisole pyrolysis and oxidation to understand tar formation during biomass combustion and gasification, Combust. Flame 161 (2014) 1474-1488.
[13] W. Yuan, T. Li, Y. Li, M. Zeng, Y. Zhang, J. Zou, C. Cao, W. Li, J. Yang, F. Qi, Experimental and kinetic modeling investigation on anisole pyrolysis: Implications on phenoxy and cyclopentadienyl chemistry, Combust. Flame 201 (2019) 187-199.
[14] C.-W. Zhou, Y. Li, U. Burke, C. Banyon, K.P. Somers, S. Ding, S. Khan, J.W. Hargis, T. Sikes, O. Mathieu, E.L. Petersen, M. AlAbbad, A. Farooq, Y. Pan, Y. Zhang, Z. Huang, J. Lopez, Z. Loparo, S.S. Vasu, H.J. Curran, An experimental and chemical kinetic modeling study of 1,3-butadiene combustion: Ignition delay time and laminar flame speed measurements, Combust. Flame 197 (2018) 423-438.
[15] Y. Pei, M. Mehl, W. Liu, T. Lu, W.J. Pitz, S. Som, A Multicomponent Blend as a Diesel Fuel Surrogate for Compression Ignition Engine Applications, J. Eng. Gas Turb. Power 137 (2015) 111502-111509.
[16] E. Ranzi, A. Frassoldati, R. Grana, A. Cuoci, T. Faravelli, A.P. Kelley, C.K. Law, Hierarchical and comparative kinetic modeling of laminar flame speeds of hydrocarbon and oxygenated fuels, Prog. Energy Combust. Sci. 38 (2012) 468-501.
[17] M. Pelucchi, C. Cavallotti, A. Cuoci, T. Faravelli, A. Frassoldati, E. Ranzi, Detailed kinetics of substituted phenolic species in pyrolysis bio-oils, React. Chem. Eng., doi:10.1039/C8RE00198G(2019).
[18] C. Lee, S. Vranckx, A. Heufer Karl, V. Khomik Sergey, Y. Uygun, H. Olivier, X. Fernandez Ravi, On the Chemical Kinetics of Ethanol Oxidation: Shock Tube, Rapid Compression Machine and Detailed Modeling Study, Z. Phys. Chem., 2012, pp. 1.
[19] S.S. Goldsborough, S. Hochgreb, G. Vanhove, M.S. Wooldridge, H.J. Curran, C.-J. Sung, Advances in rapid compression machine studies of low- and intermediate-temperature autoignition phenomena, Prog. Energy Combust. Sci. 63 (2017) 1-78.
[20] S.M. Burke, U. Burke, R. Mc Donagh, O. Mathieu, I. Osorio, C. Keesee, A. Morones, E.L. Petersen, W. Wang, T.A. DeVerter, M.A. Oehlschlaeger, B. Rhodes, R.K. Hanson, D.F. Davidson, B.W. Weber, C.-J. Sung, J. Santner, Y. Ju, F.M. Haas, F.L. Dryer, E.N. Volkov, E.J.K. Nilsson, A.A. Konnov, M. Alrefae, F. Khaled, A. Farooq, P. Dirrenberger, P.-A. Glaude, F. Battin-Leclerc, H.J. Curran, An experimental and modeling study of propene oxidation. Part 2: Ignition delay time and flame speed measurements, Combust. Flame 162 (2015) 296-314.
[21] D. Darcy, H. Nakamura, C.J. Tobin, M. Mehl, W.K. Metcalfe, W.J. Pitz, C.K. Westbrook, H.J. Curran, A high-pressure rapid compression machine study of n-propylbenzene ignition, Combust. Flame 161 (2014) 65-74.
[22] G.E. Davico, V.M. Bierbaum, C.H. DePuy, G.B. Ellison, R.R. Squires, The C-H Bond Energy of Benzene, J. Am. Chem. Soc. 117 (1995) 2590-2599.
[23] Y.-R. Luo, Comprehensive Handbook of Chemical Bond Energies, CRC PRess, Boca Raton, 2007.
[24] M.P. L. Pratali Maffei, C. Cavallotti, Private Communication, 2019.
[25] C. Saggese, A. Frassoldati, A. Cuoci, T. Faravelli, E. Ranzi, A wide range kinetic modeling study of pyrolysis and oxidation of benzene, Combust. Flame 160 (2013) 1168-1190.
[26] C.-W. Zhou, J.M. Simmie, K.P. Somers, C.F. Goldsmith, H.J. Curran, Chemical Kinetics of Hydrogen Atom Abstraction from Allylic Sites by 3O2; Implications for Combustion Modeling and Simulation, J. Phys. Chem. A 121 (2017) 1890-1899.
[27] M. Pelucchi, C. Cavallotti, T. Faravelli, S.J. Klippenstein, H-Abstraction reactions by OH, HO2, O, O2 and benzyl radical addition to O2 and their implications for kinetic modelling of toluene oxidation, PCCP 20 (2018) 10607-10627.